MHD-kinetic hybrid code based on structure-preserving finite elements with particles-in-cell

Florian Holderied[1,*], Stefan Possanner[1,2], and Xin Wang[1]

[1] *Max Planck Institute for Plasma Physics, Boltzmannstrasse 2, 85748 Garching, Germany*

[2] *Technical University of Munich, Department of Mathematics, Boltzmannstrasse 3, 85748 Garching, Germany*

[*] *Corresponding author: Florian Holderied, florian.holderied@ipp.mpg.de*

Abstract

We present a STRUcture-Preserving HYbrid code (STRUPHY) for the simulation of shear-Alfvén waves interacting with a small population of energetic particles far from thermal equilibrium (kinetic species). The code can be run either with current coupling or pressure coupling schemes; it features linearized magneto-hydrodynamic (MHD) equations, coupled nonlinearly to either full-orbit Vlasov or drift-kinetic Vlasov equations. The algorithm is based on finite element exterior calculus (FEEC) for the MHD part and particle-in-cell (PIC) methods for the kinetic part, implemented for arbitrary Riemannian metric in three space dimensions. Noise-reduction via a control variate is optional for the PIC part (δf in contrast to full-f). In the full-f version without control variate, STRUPHY is structure-preserving in the sense that it preserves the discrete energy, zero-divergence constraint and helicity up to machine precision, independent of metric and mesh parameters. Several numerical tests are presented that demonstrate this behavior.

1 Introduction

Plasma waves in magneto-hydrodynamic (MHD) fluids can be resonantly excited by energetic particles with thermal speeds in the range of the Alfvén velocity. Such wave-particle interactions are observed for instance in deuterium-tritium fusion reactors, where hot α-particles can destabilize shear Alfvén modes and thus compromise confinement time [12, 15, 8]. Another example is the interaction of fast electrons in solar wind with Earth's magnetosphere [], frequency chirping need explanations ... [] . The associated nonlinear dynamics in realistic scenarios such as fusion reactors or solar wind can be studied via computer simulation of suitable model equations. The latter range from full kinetic models of all involved plasma species (bulk and energetic particles), over hybrid codes to reduced fluid simulations, all compared in a recent benchmark study [13]. The notion of a "hybrid code" implies the following two crucial features:

1. Use of reduced model equations for bulk plasma (for instance fluid instead of kinetic).
2. Fully self-consistent description of nonlinear dynamics (beyond the linear phase).

Examples of successful implementations of hybrid codes are MEGA [21], M3D-K [4, 18], HMGC [5] and HMGC-X [23]. The appeal of hybrid codes is three-fold: a) reduced numerical cost compared to fully kinetic simulations, b) inclusion of non-equilibrium dynamics (wave-particle resonances) compared to pure fluid simulations and c) possibility of direct comparison with analytic computations (for linear dynamics). The drawback is the increased complexity of model equations. For instance, while the geometric structure (ie. Poisson bracket and/or variational principle) of MHD equations has been known for decades [17], the underlying structure of MHD-kinetic hybrid models has been discovered only very recently [22, 6]. This shows that the proper derivation of MHD-kinetic hybrids that respect fundamental physics principles such as energy conservation is a non-trivial task. As a consequence,

little attention had been paid to these issues during the design of the first generation of hybrid codes mentioned above.

In parallel to the theoretical discoveries on how to construct proper hybrid models came the advent of geometric (or structure-preserving) methods for plasma equations, see [16] for a review. These obey many of the conservation properties implied by the geometric structure on the discrete level, such as energy, charge or momentum. The main idea is to discretize directly the underlying Poisson structure or variational principle, thus transferring geometric properties to a finite-dimensional setting. The very first structure-preserving geometric PIC algorithm was designed and implemented by Squire et al. in 2012 [20]. Similar methods have later been successfully applied to Vlasov-Maxwell [10, 19, 26, 25], Vlasov-Darwin [7] and Vlasov-Poisson equations [9, 24]. The first structure-preserving geometric PIC algorithm using finite element exterior calculus (FEEC) was designed by He et al. in 2016 [11]. The same approach has later been taken by Kraus et al. [14] who used B-spline basis functions to efficiently build the discrete deRham complex, which contains Nédélec and Raviart-Thomas spaces. The theoretical foundation of FEEC has been laid by Arnold et al. [3, 1]; the interested reader may consult the recent book of Arnold [2] for a comprehensive overview.

In this work we apply the ideas of structure-preserving integration to MHD-kinetic hybrid models, namely the Hamiltonian current-coupling (CC) and pressure coupling (PC) schemes [22], respectively. In the version of the code presented here, we linearize the MHD part and focus on the nonlinear coupling to the kinetic species, which acts back on the bulk plasma via charge and current densities (CC), or via the pressure tensor (PC). FEEC is used for the discretization of the MHD part in three space dimensions and PIC for the kinetic part. We discretize the equations rather than the variational principle or the Poisson bracket, in order to avoid unnecessary abstraction. Moreover, the linearized MHD equations might lose their Hamiltonian structure if the magnetic background field is not chosen properly. In this case there is no such thing as a Poisson bracket or variational formulation, but our method of discretization still applies. In the semi-discrete setting with continuous time variable, we arrive at a non-canonical Hamiltonian system of ordinary differential equations with skew-symmetric Poisson matrix[1], which directly implies conservation of energy. The conservation of zero-divergence and helicity follow from the proper choice of FEEC spaces (Nédélec and Raviart-Thomas). The conservation laws are satisfied independent of the chosen metric and mesh parameters thanks to the separation between topological and metric properties in the theory of differential forms, upon which FEEC is built. We then use Poisson splitting and show that the described conservation laws translate to the fully discrete setting.

The article is organized as follows: ....

2 Full model and model reduction

We consider a hybrid kinetic-MHD model where the coupling of the fluid and kinetic species is done via a current coupling scheme. In classical vector calculus notation the model reads

$$\frac{\partial \rho}{\partial t} + \nabla \cdot (\rho \mathbf{U}) = 0, \tag{2.1}$$

$$\frac{\partial \mathbf{U}}{\partial t} + (\mathbf{U} \cdot \nabla)\mathbf{U} = \frac{1}{\rho}(\nabla \times \mathbf{B} + \rho_{\mathrm{h}}\mathbf{U} - \mathbf{j}_{\mathrm{h}}) \times \mathbf{B} - \frac{\nabla p}{\rho}, \tag{2.2}$$

$$\frac{\partial \mathbf{B}}{\partial t} = \nabla \times (\mathbf{U} \times \mathbf{B}), \tag{2.3}$$

$$\frac{\partial p}{\partial t} + \nabla \cdot (p\mathbf{U}) + (\gamma - 1)p\nabla \cdot \mathbf{U} = 0, \tag{2.4}$$

$$\frac{\partial f_{\mathrm{h}}}{\partial t} + \mathbf{v} \cdot \nabla f_{\mathrm{h}} + (\mathbf{B} \times \mathbf{U} + \mathbf{v} \times \mathbf{B}) \cdot \nabla_{\mathbf{v}} f_{\mathrm{h}} = 0, \tag{2.5}$$

$$\rho_{\mathrm{h}} = \int f_{\mathrm{h}} \mathrm{d}^3 v, \qquad \mathbf{j}_{\mathrm{h}} = \int \mathbf{v} f_{\mathrm{h}} \mathrm{d}^3 v. \tag{2.6}$$

[1] We cannot prove the Jacobi identity of the Poisson matrix, but speak of a Hamiltonian system anyway to guide ideas.

where we set all physical constants equal to one[2]. This set of equations forms a closed system of nonlinear partial differential equations for the the bulk mass density ρ, the bulk velocity $\mathbf{U}$, the magnetic induction $\mathbf{B}$ (which we will simply refer to as magnetic field), the bulk pressure p and the distribution function of the hot ions f_h. Furthermore, $\gamma = 5/3$ is the adiabatic exponent. This system possesses a Hamiltonian structure with the following conserved energy:

$$\mathcal{H}_0(t) = \frac{1}{2}\int \rho \mathbf{U}^2 \mathrm{d}^3x + \frac{1}{\gamma - 1}\int p \mathrm{d}^3x + \frac{1}{2}\int \mathbf{B}^2 \mathrm{d}^3x + \frac{1}{2}\int\int \mathbf{v}^2 f_\mathrm{h} \mathrm{d}^3v \mathrm{d}^3x. \tag{2.7}$$

In order to start from a simpler model we shall restrict ourselves for the moment on waves which are non-perturbative in density and pressure. Hence we drop equations (2.1) and (2.4). Moreover, we linearize all terms related to the MHD part by assuming that MHD waves are small perturbations about an equilibrium state. Making the Ansatzes $\mathbf{B} = \mathbf{B}_\mathrm{eq} + \tilde{\mathbf{B}}$, $\mathbf{U} = \tilde{\mathbf{U}}$ and $\rho = \rho_\mathrm{eq}$ and neglecting nonlinear terms in the MHD part yields

$$\rho_\mathrm{eq}\frac{\partial \tilde{\mathbf{U}}}{\partial t} = (\nabla \times \tilde{\mathbf{B}}) \times \mathbf{B}_\mathrm{eq} + (\nabla \times \mathbf{B}_\mathrm{eq}) \times \tilde{\mathbf{B}} + (\rho_\mathrm{h}\tilde{\mathbf{U}} - \mathbf{j}_\mathrm{h}) \times \mathbf{B}, \tag{2.8}$$

$$\frac{\partial \tilde{\mathbf{B}}}{\partial t} = \nabla \times (\tilde{\mathbf{U}} \times \mathbf{B}_\mathrm{eq}), \tag{2.9}$$

$$\frac{\partial f_\mathrm{h}}{\partial t} + \mathbf{v} \cdot \nabla f_\mathrm{h} + (\mathbf{B} \times \mathbf{U} + \mathbf{v} \times \mathbf{B}) \cdot \nabla_\mathbf{v} f_\mathrm{h} = 0. \tag{2.10}$$

The linearization of the MHD part breaks energy conservation, i.e. the Hamiltonian (2.7) is no longer conserved. However, we can write down the new Hamiltonian

$$\mathcal{H}_1(t) = \frac{1}{2}\int \rho_\mathrm{eq} \tilde{\mathbf{U}}^2 \mathrm{d}^3x + \frac{1}{2}\int \tilde{\mathbf{B}}^2 \mathrm{d}^3x + \frac{1}{2}\int\int \mathbf{v}^2 f_\mathrm{h} \mathrm{d}^3v \mathrm{d}^3x, \tag{2.11}$$

which is conserved if $\nabla \times \mathbf{B}_\mathrm{eq} = 0$.

We shall use classical particle-in-cell techniques for solving the kinetic equation (2.10) and the framework of *finite element exterior calculus* (FEEC) for solving field equations. In the latter, one works with differential forms rather than vector and scalar field. This allows us to treat arbitrary geometries in a natural fashion. For physical reasons we assume the bulk mass density and the hot charge density to be 3-forms ($\rho_\mathrm{eq}, \rho_\mathrm{h} \to \rho^3_\mathrm{eq}, \rho^3_\mathrm{h}$), the magnetic field to be a 2-form ($\mathbf{B}_\mathrm{eq}, \tilde{\mathbf{B}} \to B^2_\mathrm{eq}, \tilde{B}^2$) and the bulk velocity and the hot current density to be 1-forms ($\tilde{\mathbf{U}}, \mathbf{j}_\mathrm{h} \to \tilde{U}^1, j^1_\mathrm{h}$). Eq. (2.8) and (2.9) can then be written as

$$(*\rho^3_\mathrm{eq}) \wedge \frac{\partial \tilde{U}^1}{\partial t} = i_{\#*B^2_\mathrm{eq}} \mathrm{d} * \tilde{B}^2 + i_{\#*\tilde{B}^2} \mathrm{d} * B^2_\mathrm{eq} - (*\rho^3_\mathrm{h}) \wedge i_{\#\tilde{U}^1} B^2 + i_{\#j^1_\mathrm{h}} B^2, \tag{2.12}$$

$$\frac{\partial \tilde{B}^2}{\partial t} + \mathrm{d}(i_{\#U^1} B^2_\mathrm{eq}) = 0, \tag{2.13}$$

where $*$ is the Hodge-star operator, $\wedge$ the wedge product, i the interior product and $\#$ the sharp operator which transforms a 1-form to a vector field.

3 Semi-discretization in space

As a next step, we introduce finite element basis functions which satisfy a discrete deRham sequence and which form a commuting diagram with the continuous functions via the interpolation-histopolation projectors Π_0, Π_1, Π_2 and Π_3. This is depicted in Fig. 1. Assuming that we know the basis functions in each space (how this can be done with e.g. tensor-product B-splines, see Sec. ...), we express the forms in their respective bases as

$$\tilde{U}^1(\mathbf{q}) \approx \tilde{U}^1_h(\mathbf{q}) = \sum_\mathbf{i}\sum_{\mu=1}^3 u_{\mu,\mathbf{i}} \Lambda^1_{\mu,\mathbf{i}}(\mathbf{q}) \mathrm{d}q^\mu, \qquad \mathbf{u}^\top := (\mathbf{u}_1^\top, \mathbf{u}_2^\top, \mathbf{u}_3^\top) \in \mathbb{R}^{3N}, \tag{3.1}$$

$$\tilde{B}^2(\mathbf{q}) \approx \tilde{B}^2_h(\mathbf{q}) = \sum_\mathbf{i}\sum_{\mu=1}^3 b_{\mu,\mathbf{i}} \Lambda^2_{\mu,\mathbf{i}}(\mathbf{q}) (\mathrm{d}q^\alpha \wedge \mathrm{d}q^\beta)_\mu, \qquad \mathbf{b}^\top := (\mathbf{b}_1^\top, \mathbf{b}_2^\top, \mathbf{b}_3^\top) \in \mathbb{R}^{3N}, \tag{3.2}$$

[2]We assume hot ions with a positive charge. Therefore, one does not have to be careful with the signs in (2.6)

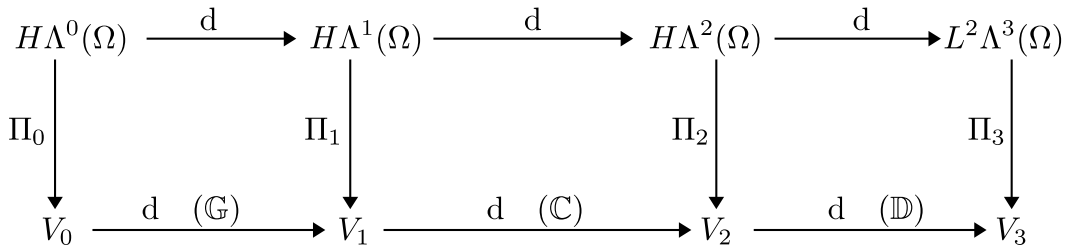

Figure 1: Commuting diagram for function spaces in 3d. The upper line represents the de Rham sequence for the continuous spaces, while the lower line represents the discrete counterpart.

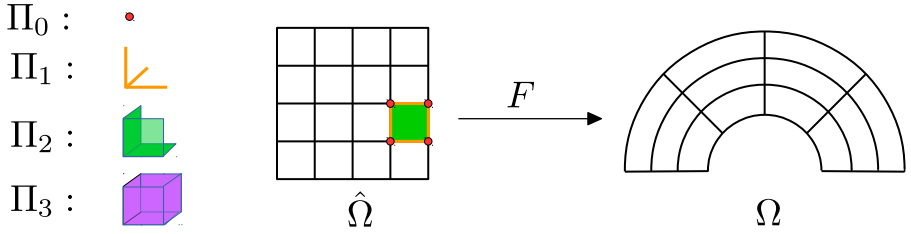

Figure 2: Commuting projectors. Unlike classical finite element methods, the degrees of freedom do not only represent point values, but also edge integrals, face integrals and volume integrals.

where $\mathbf{i} = (i_1, i_2, i_3)$ is a multi-index and N the total number of basis functions. To simplify the notation, we write for the components of the differential forms

$$\tilde{U}_h^1 \leftrightarrow \tilde{\mathbf{U}}_h^\top = (\mathbf{u}_1^\top, \mathbf{u}_2^\top, \mathbf{u}_3^\top) \begin{pmatrix} \mathbf{\Lambda}_1^1 & 0 & 0 \\ 0 & \mathbf{\Lambda}_2^1 & 0 \\ 0 & 0 & \mathbf{\Lambda}_3^1 \end{pmatrix} = \mathbf{u}^\top \mathbb{\Lambda}^1, \qquad \mathbb{\Lambda}^1 \in \mathbb{R}^{3N\times 3}, \tag{3.3}$$

$$\tilde{B}_h^2 \leftrightarrow \tilde{\mathbf{B}}_h^\top = (\mathbf{b}_1^\top, \mathbf{b}_2^\top, \mathbf{b}_3^\top) \begin{pmatrix} \mathbf{\Lambda}_1^2 & 0 & 0 \\ 0 & \mathbf{\Lambda}_2^2 & 0 \\ 0 & 0 & \mathbf{\Lambda}_3^2 \end{pmatrix} = \mathbf{b}^\top \mathbb{\Lambda}^2, \qquad \mathbb{\Lambda}^2 \in \mathbb{R}^{3N\times 3}. \tag{3.4}$$

As already stated, we solve the kinetic equation with particle-in-cell techniques. Hence we assume a particle-like distribution function which, in physical space, takes the form

$$f_\mathrm{h} = f_\mathrm{h}(t, \mathbf{x}, \mathbf{v}) \approx \sum_k w_k \delta(\mathbf{x} - \mathbf{x}_k(t)) \delta(\mathbf{v} - \mathbf{v}_k(t)). \tag{3.5}$$

From this, the hot ion charge density, current density and energy density can easily be obtained by taking the first three moments in velocity space:

$$\mathring{\rho}_\mathrm{h}(t, \mathbf{x}) = \sum_k w_k \delta(\mathbf{x} - \mathbf{x}_k(t)), \tag{3.6}$$

$$\mathring{\mathbf{j}}_\mathrm{h}(t, \mathbf{x}) = \sum_k w_k \delta(\mathbf{x} - \mathbf{x}_k(t)) \mathbf{v}_k(t), \tag{3.7}$$

$$\mathring{\epsilon}_\mathrm{h}(t, \mathbf{x}) = \sum_k w_k \delta(\mathbf{x} - \mathbf{x}_k(t)) \mathbf{v}_k^2(t). \tag{3.8}$$

To avoid confusions, we use the notation $\mathring{(\cdot)}$, where necessary, for quantities which are defined on the physical space. Since there is no difference between vectors/scalars and forms in physical space, these expressions are as well the components of the 3-form number density, the 1-form current density and the 3-form energy density. To get the components on the logical domain we apply the transformation

formulas for 3-forms, respectively 1-forms to obtain

$$\rho_{\mathrm{h},123}(t,\mathbf{q}) = \sqrt{g}\mathring{\rho}_{\mathrm{h}}(t,F(\mathbf{q})) = \sum_k w_k \delta(\mathbf{q}-\mathbf{q}_k(t)), \tag{3.9}$$

$$\mathbf{j}_{\mathrm{h}}(t,\mathbf{q}) = DF^{\top}\mathring{\mathbf{j}}_{\mathrm{h}}(t,F(\mathbf{q})) = \frac{1}{\sqrt{g}}DF^{\top}\sum_k w_k \delta(\mathbf{q}-\mathbf{q}_k(t))\mathbf{v}_k(t), \tag{3.10}$$

$$\epsilon_{\mathrm{h},123}(t,\mathbf{q}) = \sqrt{g}\mathring{\epsilon}_{\mathrm{h}}(t,F(\mathbf{q})) = \sum_k w_k \delta(\mathbf{q}-\mathbf{q}_k(t))\mathbf{v}_k^2(t), \tag{3.11}$$

where we made use of the transformation formula

$$\delta(\mathbf{x}-\mathbf{x}_k(t)) = \frac{1}{\sqrt{g}}\delta(\mathbf{q}-\mathbf{q}_k(t)). \tag{3.12}$$

Let us use these results to derive an energy conserving semi-discrete system for the finite element coefficients of $\tilde{U}_h^1$ and $\tilde{B}_h^2$ and the particle's positions $(\mathbf{q}_k)_{k=1,\dots,N_{\mathrm{p}}}$ and velocities $(\mathbf{v}_k)_{k=1,\dots,N_{\mathrm{p}}}$.

3.1 Momentum equation

We choose a weak formulation for the momentum equation and consequently take the inner product with a test function $C^1 \in H\Lambda^1(\Omega)$ to obtain the variational formulation: Find $\tilde{U}^1 \in H\Lambda^1(\Omega)$ such that

$$\left((*\rho_{\mathrm{eq}}^3)\wedge\frac{\partial\tilde{U}^1}{\partial t}, C^1\right) = \left(i_{\#*B_{\mathrm{eq}}^2}\mathrm{d}*\tilde{B}^2, C^1\right) + \left(i_{\#*\tilde{B}^2}\mathrm{d}*B_{\mathrm{eq}}^2, C^1\right) \tag{3.13}$$

$$- \left((*\rho_{\mathrm{h}}^3)\wedge i_{\#\tilde{U}^1}B^2, C^1\right) + \left(i_{\#j_{\mathrm{h}}^1}B^2, C^1\right) \qquad \forall\, C^1 \in H\Lambda^1(\Omega). \tag{3.14}$$

We apply the Galerkin approximation to each term and project back into the right spaces where necessary. Let us start with the first term on the left-hand side involving the equilibrium bulk density. To achieve conservation of energy at the discrete level we make use of the fact that the wedge with a 0-form is just a multiplication with a scalar. Hence the wedge product can as well be applied to the test function and the following equality holds:

$$\left((*\rho_{\mathrm{eq}}^3)\wedge\frac{\partial\tilde{U}^1}{\partial t}, C^1\right) = \frac{1}{2}\left((*\rho_{\mathrm{eq}}^3)\wedge\frac{\partial\tilde{U}^1}{\partial t}, C^1\right) + \frac{1}{2}\left(\frac{\partial\tilde{U}^1}{\partial t}, (*\rho_{\mathrm{eq}}^3)\wedge C^1\right). \tag{3.15}$$

Using the definition of the inner product of 1-forms yields for the first term

$$\left((*\rho_{\mathrm{eq}}^3)\wedge\frac{\partial\tilde{U}^1}{\partial t}, C^1\right) = \int_{\hat{\Omega}}\frac{1}{\sqrt{g}}\rho_{\mathrm{eq},123}\dot{\tilde{\mathbf{U}}}^{\top}G^{-1}\mathbf{C}\sqrt{g}\,\mathrm{d}^3q \approx \int_{\hat{\Omega}}\Pi_1\left(\frac{1}{\sqrt{g}}\rho_{\mathrm{eq},123}\dot{\tilde{\mathbf{U}}}_h^{\top}\right)G^{-1}\mathbf{C}_h\sqrt{g}\,\mathrm{d}^3q \tag{3.16}$$

$$= \dot{\mathbf{u}}^{\top}\mathcal{W}^{\top}\underbrace{\int_{\hat{\Omega}}\mathbb{\Lambda}^1 G^{-1}(\mathbb{\Lambda}^1)^{\top}\sqrt{g}\,\mathrm{d}^3q}_{=:\mathbb{M}^1}\mathbf{c} = \dot{\mathbf{u}}^{\top}\mathcal{W}^{\top}\mathbb{M}^1\mathbf{c} \quad \forall\,\mathbf{c}\in\mathbb{R}^{3N}, \tag{3.17}$$

where $\mathbb{M}^1 \in \mathbb{R}^{3N\times 3N}$ is the mass matrix in the space V_1. The projection matrix, for which we use calligraphic symbols, is given by

$$\mathcal{W}_{ij} = \Pi_{1,\mu}^{i_\mu}\left[\frac{1}{\sqrt{g}}\rho_{\mathrm{eq},123}\mathbb{\Lambda}_{j_\mu}^1\right], \qquad i = \begin{cases} i_\mu, & \mu = 1 \\ N+i_\mu, & \mu = 2 \\ 2N+i_\mu, & \mu = 3 \end{cases} \tag{3.18}$$

for $i_\mu = \{1,\dots,N\}$. Unfortunately, this matrix is dense which is problematic from a memory consumption point of view. Therefore, we just compute the right-hand sides of the projection for each basis

function which defines a sparse matrix due to the compact support of B-splines. The final projection we then perform in each time step again. Explicitly, the right-hand side reads

$$\tilde{\mathcal{W}} := \begin{pmatrix} \mathrm{vec}_{1,1}\left[\rho_{\mathrm{eq}}/\sqrt{g}(\boldsymbol{\Lambda}_1^1)^\top\right] & 0 & 0 \\ 0 & \mathrm{vec}_{1,2}\left[\rho_{\mathrm{eq}}/\sqrt{g}(\boldsymbol{\Lambda}_2^1)^\top\right] & 0 \\ 0 & 0 & \mathrm{vec}_{1,3}\left[\rho_{\mathrm{eq}}/\sqrt{g}(\boldsymbol{\Lambda}_3^1)^\top\right] \end{pmatrix} \tag{3.19}$$

$$\boldsymbol{\mathcal{I}}_1^{-1} := \begin{pmatrix} \mathcal{I}_{1,1}^{-1} & 0 & 0 \\ 0 & \mathcal{I}_{1,2}^{-1} & 0 \\ 0 & 0 & \mathcal{I}_{1,3}^{-1} \end{pmatrix}, \tag{3.20}$$

$$\Rightarrow \quad \mathcal{W} = \boldsymbol{\mathcal{I}}_1^{-1}\tilde{\mathcal{W}}. \tag{3.21}$$

For some 1-form $f^1 = f_1 \mathrm{d}q^1 + f_2 \mathrm{d}q^2 + f_3 \mathrm{d}q^3$ the projection is a mixed interpolation-histopolation problem defined by

$$(\mathrm{vec}_{1,1})_i(f^1) = \int_{\xi_{i_1}}^{\xi_{i_1+1}} f_1(q_1, \xi_{i_2}, \xi_{i_3})\mathrm{d}q^1, \qquad (\mathcal{I}_{1,1})_{ij} = \int_{\xi_{i_1}}^{\xi_{i_1+1}} \Lambda^1_{1,j}(q_1, \xi_{i_2}, \xi_{i_3})\mathrm{d}q^1 \tag{3.22}$$

$$(\mathrm{vec}_{1,2})_i(f^1) = \int_{\xi_{i_2}}^{\xi_{i_2+1}} f_2(\xi_{i_1}, q_2, \xi_{i_3})\mathrm{d}q^2, \qquad (\mathcal{I}_{1,2})_{ij} = \int_{\xi_{i_2}}^{\xi_{i_2+1}} \Lambda^1_{2,j}(\xi_{i_1}, q_2, \xi_{i_3})\mathrm{d}q^2 \tag{3.23}$$

$$(\mathrm{vec}_{1,3})_i(f^1) = \int_{\xi_{i_3}}^{\xi_{i_3+1}} f_3(\xi_{i_1}, \xi_{i_2}, q_3)\mathrm{d}q^3, \qquad (\mathcal{I}_{1,3})_{ij} = \int_{\xi_{i_3}}^{\xi_{i_3+1}} \Lambda^1_{3,j}(\xi_{i_1}, \xi_{i_2}, q_3)\mathrm{d}q^3, \tag{3.24}$$

where the $\xi_{\mathbf{i}}$ are some well-chosen interpolation points on the logical domain. Finally, we obtain

$$\left((*\rho^3_{\mathrm{eq}}) \wedge \frac{\partial \tilde{U}^1}{\partial t}, C^1\right) \approx \frac{1}{2}\mathbf{c}^\top \left(\mathbb{M}^1\mathcal{W} + \mathcal{W}^\top\mathbb{M}^1\right)\dot{\mathbf{u}} =: \mathbf{c}^\top\mathcal{A}\dot{\mathbf{u}}, \tag{3.25}$$

with $\mathcal{A} \in \mathbb{R}^{3N\times 3N}$ being symmetric.

Using the identities $\langle i_{\#\gamma^1}\alpha^2, \beta^1\rangle = \langle \alpha^2, \gamma^1 \wedge \beta^1\rangle$ and $*(*\alpha^2 \wedge \beta^1) = i_{\#\beta^1}\alpha^2$, the first term on the right-hand side can be written as

$$\left(i_{\#*B^2_{\mathrm{eq}}}\mathrm{d} * \tilde{B}^2, C^1\right) = \left(d * \tilde{B}^2, *B^2_{\mathrm{eq}} \wedge C^1\right) = \left(*\mathrm{d} * \tilde{B}^2, *(*B^2_{\mathrm{eq}} \wedge C^1)\right) = \left(d^*\tilde{B}^2, i_{\#C^1}B^2_{\mathrm{eq}}\right), \tag{3.26}$$

where we introduced the co-differential operator $\mathrm{d}^*\alpha^p = (-1)^p * \mathrm{d} * \alpha^p$. Applying the Green formula for differential forms and assuming that the boundary term vanishes yields

$$\left(i_{\#*B^2_{\mathrm{eq}}}\mathrm{d} * \tilde{B}^2, C^1\right) = \left(\tilde{B}^2, \mathrm{d}i_{\#C^1}B^2_{\mathrm{eq}}\right) = \int_{\hat{\Omega}} \frac{1}{g}\hat{\hat{\mathbf{B}}}^\top G\left(\nabla \times (\hat{\mathbf{B}}_{\mathrm{eq}} \times G^{-1}\mathbf{C})\right)\sqrt{g}\,\mathrm{d}^3q \tag{3.27}$$

$$\approx \mathbf{b}^\top \underbrace{\int_{\hat{\Omega}} \frac{1}{\sqrt{g}}\mathbb{\Lambda}^2 G(\mathbb{\Lambda}^2)^\top \mathrm{d}^3q}_{=:\mathbb{M}^2}\, \mathbb{C}\tilde{\Pi}_1\left(\mathbb{B}_{\mathrm{eq}}G^{-1}(\mathbb{\Lambda}^1)^\top\right)\mathbf{c} = \mathbf{b}^\top\mathbb{M}^2\mathbb{C}\mathcal{T}\mathbf{c} \quad \forall \mathbf{c} \in \mathbb{R}^{3N}, \tag{3.28}$$

where we introduced the discrete curl matrix $\mathbb{C} \in \mathbb{R}^{3N\times 3N}$, the mass matrix $\mathbb{M}^2 \in \mathbb{R}^{3N\times 3N}$ in the space V_2 and we wrote the vector product of the background magnetic field with the velocity field in terms of a matrix-vector product by using the matrix

$$\mathbb{B}_{\mathrm{eq}} = \begin{pmatrix} 0 & -B_{\mathrm{eq},12} & B_{\mathrm{eq},31} \\ B_{\mathrm{eq},12} & 0 & -B_{\mathrm{eq},23} \\ -B_{\mathrm{eq},31} & B_{\mathrm{eq},23} & 0 \end{pmatrix} \in \mathbb{R}^{3\times 3}. \tag{3.29}$$

The projection matrix $\mathcal{T}$ is given by

$$\mathcal{T}_{ij} := \Pi^{i_\mu}_{1,\mu}\left[(\mathbb{B}_{\mathrm{eq}})_{\mu k}G^{kl}\Lambda^1_{j,l}\right] = \Pi^{i_\mu}_{1,\mu}\left[\epsilon_{\mu mk}B_{\mathrm{eq},m}G^{kl}\Lambda^1_{j,l}\right], \qquad \mu = \{1,2,3\}, \tag{3.30}$$

which has the right-hand sides

$$\tilde{\mathcal{T}} = \tag{3.31}$$

$$= \begin{pmatrix} \mathrm{vec}_{1,1}\left[(B_{\mathrm{eq},31}G^{31} - B_{\mathrm{eq},12}G^{21})(\mathbf{\Lambda}_1^1)^\top, (B_{\mathrm{eq},31}G^{32} - B_{\mathrm{eq},12}G^{22})(\mathbf{\Lambda}_2^1)^\top, (B_{\mathrm{eq},31}G^{33} - B_{\mathrm{eq},12}G^{23})(\mathbf{\Lambda}_3^1)^\top\right] \\ \mathrm{vec}_{1,2}\left[(B_{\mathrm{eq},12}G^{11} - B_{\mathrm{eq},23}G^{31})(\mathbf{\Lambda}_1^1)^\top, (B_{\mathrm{eq},12}G^{12} - B_{\mathrm{eq},23}G^{32})(\mathbf{\Lambda}_2^1)^\top, (B_{\mathrm{eq},12}G^{13} - B_{\mathrm{eq},23}G^{33})(\mathbf{\Lambda}_3^1)^\top\right] \\ \mathrm{vec}_{1,3}\left[(B_{\mathrm{eq},23}G^{21} - B_{\mathrm{eq},31}G^{11})(\mathbf{\Lambda}_1^1)^\top, (B_{\mathrm{eq},23}G^{22} - B_{\mathrm{eq},31}G^{12})(\mathbf{\Lambda}_2^1)^\top, (B_{\mathrm{eq},23}G^{23} - B_{\mathrm{eq},31}G^{13})(\mathbf{\Lambda}_3^1)^\top\right] \end{pmatrix}. \tag{3.32}$$

Performing the same steps for the second term yields

$$\left(i_{\#*\tilde{B}^2}\mathrm{d} * B^2_{\mathrm{eq}}, C^1\right) = \left(B^2_{\mathrm{eq}}, \mathrm{d}i_{\#C^1}\tilde{B}^2\right) = \int_{\hat{\Omega}} \frac{1}{g}\hat{\mathbf{B}}^\top_{\mathrm{eq}} G\left(\nabla \times (\tilde{\mathbf{B}} \times G^{-1}\mathbf{C})\right)\sqrt{g}\,\mathrm{d}^3q \tag{3.33}$$

$$\approx \tilde{\Pi}_2\left(\hat{\mathbf{B}}^\top_{\mathrm{eq}}\right)\int_{\hat{\Omega}} \frac{1}{\sqrt{g}}\mathbb{\Lambda}^2 G(\mathbb{\Lambda}^2)^\top \mathrm{d}^3q\, \mathbb{C}\tilde{\Pi}_1\left[(\mathbb{\Lambda}^2)^\top\mathbf{b} \times G^{-1}(\mathbb{\Lambda}^1)^\top\mathbf{c}\right] \tag{3.34}$$

$$= \mathbf{b}^\top_{\mathrm{eq}}\mathbb{M}^2\mathbb{C}(\mathbf{b}^\top\mathcal{P}\mathbf{c}) \quad \forall \mathbf{c} \in \mathbb{R}^{3N}. \tag{3.35}$$

The projection tensor $\mathcal{P} \in \mathbb{R}^{3N\times 3N\times 3N}$ is given by

$$\mathcal{P}_{ijk} = \Pi_1^{j_\mu}\left[\epsilon_{\mu lm}\Lambda^2_{i,l}G^{mn}\Lambda^1_{k,n}\right], \tag{3.36}$$

where it is important to note that the entries of $\mathbf{b}$ contract from left with the index i and the entries of $\mathbf{c}$ from right with the index k. The result is then a vector defined by the index j.

Next, we consider the term involving the hot ion current density. Since this term must be computed from the particle-in-cell approximation of the hot ion distribution function, we can make use of a control variate M_0 for noise reduction. In practice, one can take the equilibrium distribution function which is typically a Maxwellian. By noting that a distribution function can be transformed to a 3-form by multiplying with the square root of the Jacobi determinant, we find

$$\left(i_{\#j^1_{\mathrm{h}}}B^2, C^1\right) = \int_{\hat{\Omega}} \mathbf{C}^\top G^{-1}(\hat{\mathbf{B}} \times G^{-1}\mathbf{j}_{\mathrm{h}})\sqrt{g}\,\mathrm{d}^3q \tag{3.37}$$

$$= \int_{\hat{\Omega}} \mathbf{C}^\top G^{-1}\left[\hat{\mathbf{B}} \times DF^{-1}\int (\mathring{f}_{\mathrm{h}} - \mathring{M}_0)\mathbf{v}\,\mathrm{d}^3v\right]\sqrt{g}\,\mathrm{d}^3q \tag{3.38}$$

$$+ \int_{\hat{\Omega}} \mathbf{C}^\top G^{-1}\left[\hat{\mathbf{B}} \times DF^{-1}\int \mathring{M}_0\mathbf{v}\,\mathrm{d}^3v\right]\sqrt{g}\,\mathrm{d}^3q \tag{3.39}$$

$$= \int_{\hat{\Omega}}\int \mathbf{C}^\top G^{-1}\left[\hat{\mathbf{B}} \times DF^{-1}\left(\frac{f_{\mathrm{h}} - M_0}{g_{\mathrm{h}}}\right)\mathbf{v}\right] g_{\mathrm{h}}\,\mathrm{d}^3v\,\mathrm{d}^3q + \mathbf{c}^\top\int_{\hat{\Omega}} \mathbb{\Lambda}^1 G^{-1}\left(\hat{\mathbf{B}} \times DF^{-1}\mathring{\mathbf{j}}_{\mathrm{h}0}\right)\sqrt{g}\,\mathrm{d}^3q \tag{3.40}$$

The second term is just the right-hand side of the L^2-projection in the space V^1 of the function in the curly brackets which we can compute numerically for some given magnetic field and which we denote by $\mathbf{x}_2 = \mathbf{x}_2(\mathbf{b})$. It is important to note that in this form the equilibrium current density must be given in physical space. In the first term we introduced the marker sampling density g_{h} which must is normalized to one. This allows us to interpret the integral as the expectation value of a random variable which we can approximate using the randomly drawn markers. Hence we can write

$$\int_{\hat{\Omega}}\int \mathbf{C}^\top G^{-1}\left[\hat{\mathbf{B}} \times DF^{-1}\left(\frac{f_{\mathrm{h}} - M_0}{g_{\mathrm{h}}}\right)\mathbf{v}\right] g_{\mathrm{h}}\,\mathrm{d}^3v\,\mathrm{d}^3q \tag{3.41}$$

$$\approx \sum_k \underbrace{\frac{1}{N_k}\left(\frac{f^0_{\mathrm{h}}(\mathbf{q}^0_k, \mathbf{v}^0_k)}{g^0_{\mathrm{h}}(\mathbf{q}^0_k, \mathbf{v}^0_k)} - \frac{M_0(\mathbf{q}_k, \mathbf{v}_k)}{g^0_{\mathrm{h}}(\mathbf{q}^0_k, \mathbf{v}^0_k)}\right)}_{:=w_k(t)} \mathbf{C}^\top_h(\mathbf{q}_k)G^{-1}(\mathbf{q}_k)(\hat{\mathbf{B}}_h(\mathbf{q}_k) \times DF^{-1}(\mathbf{q}_k)\mathbf{v}_k), \tag{3.42}$$

$$= \mathbf{c}^\top\mathbb{P}_1\mathbb{W}\tilde{G}^{-1}\hat{\mathbb{B}}\tilde{DF}^{-1}\mathbf{V}, \tag{3.43}$$

where we introduced the antisymmetric block matrix

$$\hat{\mathbb{B}} = \hat{\mathbb{B}}(\mathbf{b}, \mathbf{Q}) = \tag{3.44}$$

$$= \begin{pmatrix} 0 & -\mathrm{diag}[\mathbb{P}_3^{2\top}(\mathbf{Q})\mathbf{b}_3 + B_{\mathrm{eq},12}(\mathbf{Q})] & \mathrm{diag}[\mathbb{P}_2^{2\top}(\mathbf{Q})\mathbf{b}_2 + B_{\mathrm{eq},31}(\mathbf{Q})] \\ \mathrm{diag}[\mathbb{P}_3^{2\top}(\mathbf{Q})\mathbf{b}_3 + B_{\mathrm{eq},12}(\mathbf{Q})] & 0 & -\mathrm{diag}[\mathbb{P}_1^{2\top}(\mathbf{Q})\mathbf{b}_1 + B_{\mathrm{eq},23}(\mathbf{Q})] \\ -\mathrm{diag}[\mathbb{P}_2^{2\top}(\mathbf{Q})\mathbf{b}_2 + B_{\mathrm{eq},31}(\mathbf{Q})] & \mathrm{diag}[\mathbb{P}_1^{2\top}(\mathbf{Q})\mathbf{b}_1 + B_{\mathrm{eq},23}(\mathbf{Q})] & 0 \end{pmatrix}. \tag{3.45}$$

where $(\mathbb{P}^2_{1/2/3})_{ik} = \Lambda^2_{1/2/3,i}(\mathbf{q}_k) \in \mathbb{R}^{N\times N_p}$ represents the evaluation of all basis functions at all particle positions and $\mathbf{Q} \in \mathbb{R}^{3N_p}$ is the vector holding all particle positions. Moreover,

$$\mathbf{V} = (v_{1x}, v_{2x}, \dots, v_{N_p x}, v_{1y}, v_{2y}, \dots, v_{N_p y}, v_{1z}, v_{2z}, \dots, v_{N_p z})^\top \in \mathbb{R}^{3N_p}, \tag{3.46}$$

$$\mathbb{W} = \begin{pmatrix} \mathrm{diag}(w_1, \dots, w_{N_p}) & & \\ & \mathrm{diag}(w_1, \dots, w_{N_p}) & \\ & & \mathrm{diag}(w_1, \dots, w_{N_p}) \end{pmatrix} \in \mathbb{R}^{3N_p\times 3N_p}, \tag{3.47}$$

$$\mathbb{P}^1 = \mathbb{P}^1(\mathbf{Q}) = \begin{pmatrix} \mathbb{P}^1_1(\mathbf{Q}) & & \\ & \mathbb{P}^1_2(\mathbf{Q}) & \\ & & \mathbb{P}^1_3(\mathbf{Q}) \end{pmatrix} \in \mathbb{R}^{3N\times 3N_p}. \tag{3.48}$$

$$\tilde{G}^{-1} = \tilde{G}^{-1}(\mathbf{Q}) = \begin{pmatrix} \mathrm{diag}(G^{11}(\mathbf{Q})) & \mathrm{diag}(G^{12}(\mathbf{Q})) & \mathrm{diag}(G^{13}(\mathbf{Q})) \\ \mathrm{diag}(G^{21}(\mathbf{Q})) & \mathrm{diag}(G^{22}(\mathbf{Q})) & \mathrm{diag}(G^{23}(\mathbf{Q})) \\ \mathrm{diag}(G^{31}(\mathbf{Q})) & \mathrm{diag}(G^{32}(\mathbf{Q})) & \mathrm{diag}(G^{33}(\mathbf{Q})) \end{pmatrix} \in \mathbb{R}^{3N_p\times 3N_p}, \tag{3.49}$$

$$\tilde{DF^{-1}} = \tilde{DF^{-1}}(\mathbf{Q}) = \begin{pmatrix} \mathrm{diag}(DF^{11}(\mathbf{Q})) & \mathrm{diag}(DF^{12}(\mathbf{Q})) & \mathrm{diag}(DF^{13}(\mathbf{Q})) \\ \mathrm{diag}(DF^{21}(\mathbf{Q})) & \mathrm{diag}(DF^{22}(\mathbf{Q})) & \mathrm{diag}(DF^{23}(\mathbf{Q})) \\ \mathrm{diag}(DF^{31}(\mathbf{Q})) & \mathrm{diag}(DF^{32}(\mathbf{Q})) & \mathrm{diag}(DF^{33}(\mathbf{Q})) \end{pmatrix} \in \mathbb{R}^{3N_p\times 3N_p}. \tag{3.50}$$

Finally, the term involving the hot ion charge density amounts to

$$\left((*\rho^3_{\mathrm{h}}) \wedge i_{\#\tilde{U}^1} B^2, C^1\right) = \int_{\hat{\Omega}} \mathbf{C}^\top G^{-1} \left(\mathring{\rho}_{\mathrm{h}} \hat{\mathbf{B}} \times G^{-1}\tilde{\mathbf{U}}\right) \sqrt{g}\, \mathrm{d}^3 q \tag{3.51}$$

$$= \int_{\hat{\Omega}} \mathbf{C}^\top G^{-1} \left(\int (\mathring{f}^0_{\mathrm{h}} - \mathring{M}_0)\, \mathrm{d}^3 v\, \hat{\mathbf{B}} \times G^{-1}\tilde{\mathbf{U}}\right) \sqrt{g}\, \mathrm{d}^3 q \tag{3.52}$$

$$+ \int_{\hat{\Omega}} \mathbf{C}^\top G^{-1} \left(\int \mathring{M}_0\, \mathrm{d}^3 v\, \hat{\mathbf{B}} \times G^{-1}\tilde{\mathbf{U}}\right) \sqrt{g}\, \mathrm{d}^3 q \tag{3.53}$$

$$\approx \sum_k w_k \mathbf{C}^\top_h(\mathbf{q}_k) G^{-1}(\mathbf{q}_k)(\hat{\mathbf{B}}_h(\mathbf{q}_k) \times G^{-1}(\mathbf{q}_k)\tilde{\mathbf{U}}_h(\mathbf{q}_k)) \tag{3.54}$$

$$+ \int_{\hat{\Omega}} \mathbf{C}^\top G^{-1} \left(\rho_{\mathrm{h}0,123}\, \hat{\mathbf{B}} \times G^{-1}\tilde{\mathbf{U}}\right) \mathrm{d}^3 q \tag{3.55}$$

$$= \mathbf{c}^\top \mathbb{P}_1 \mathbb{W} \tilde{G}^{-1} \hat{\mathbb{B}} \tilde{G}^{-1} \mathbb{P}_1^\top \mathbf{u} + \mathbf{c}^\top X_1(\mathbf{b})\mathbf{u}, \tag{3.56}$$

where both terms are clearly antisymmetric because $\hat{\mathbb{B}}$ is antisymmetric. In total we get the following semi-discrete momentum balance equation:

$$\mathcal{A}\dot{\mathbf{u}} = \mathcal{T}^\top \mathbb{C}^\top \mathbb{M}^2 \mathbf{b} + \mathbf{b}^\top_{\mathbf{eq}} \mathbb{M}^2 \mathbb{C} \mathcal{P}^{jki} \mathbf{b} - \mathbb{P}_1 \mathbb{W} \tilde{G}^{-1} \hat{\mathbb{B}} \tilde{G}^{-1} \mathbb{P}_1^\top \mathbf{u} - X_1 \mathbf{u} + \mathbb{P}_1 \mathbb{W} \tilde{G}^{-1} \hat{\mathbb{B}} \tilde{DF^{-1}} \mathbf{V} + \mathbf{x}_2 \tag{3.57}$$

where $\mathcal{P}^{jki}$ means that order of the indices is changed from $()_{ijk}$ to $()_{jki}$ such that $\mathbf{b}$ still contracts with the index i from right and the $\mathbb{C}$ with the index j from left.

3.2 Induction equation

In contrast to the momentum equation, we keep the induction equation in strong form. This time we have to use the projector Π_2 which commutes with the curl operator:

$$\frac{\partial \tilde{\mathbf{B}}_h}{\partial t} + \Pi_2 \left[\nabla \times (\hat{\mathbf{B}}_{\mathrm{eq}} \times G^{-1}\tilde{\mathbf{U}}_h)\right] = 0 \tag{3.58}$$

$$\Leftrightarrow \quad \frac{\partial \mathbf{b}}{\partial t} + \mathbb{C}\tilde{\Pi}_1 \left[\mathbb{B}_{\mathrm{eq}} G^{-1} (\mathbb{\Lambda}^1)^\top\right] \mathbf{u} = 0 \tag{3.59}$$

$$\Leftrightarrow \quad \frac{\partial \mathbf{b}}{\partial t} + \mathbb{C}\mathcal{T}\mathbf{u} = 0. \tag{3.60}$$

We immediately see that we obtain the same projection matrix as for the Hall term in the momentum equation.

3.3 Particles' equation of motion

As a last step, the equations of motion for a single particle with logical coordinate $\mathbf{q}_k$ and physical velocity $\mathbf{v}_k$ read

$$\frac{\mathrm{d}\mathbf{q}_k}{\mathrm{d}t} = DF^{-1}(\mathbf{q}_k)\mathbf{v}_k, \tag{3.61}$$

$$\frac{\mathrm{d}\mathbf{v}_k}{\mathrm{d}t} = \frac{1}{\sqrt{g}}DF(\mathbf{q}_k)\hat{\mathbf{B}}_h(\mathbf{q}_k) \times DF^{-\top}(\mathbf{q}_k)\mathbf{U}_h(\mathbf{q}_k) - \frac{1}{\sqrt{g}}DF(\mathbf{q}_k)\hat{\mathbf{B}}_h(\mathbf{q}_k) \times \mathbf{v}_k. \tag{3.62}$$

$$= DF^{-\top}(\mathbf{q}_k)(\hat{\mathbf{B}}_h(\mathbf{q}_k) \times G^{-1}(\mathbf{q}_k)\mathbf{U}_h(\mathbf{q}_k)) - DF^{-\top}(\mathbf{q}_k)(\hat{\mathbf{B}}_h(\mathbf{q}_k) \times DF^{-1}\mathbf{v}_k), \tag{3.63}$$

where we used the identity $A\mathbf{b} \times A\mathbf{c} = \det(A)A^{-\top}(\mathbf{b} \times \mathbf{c})$ from vector calculus. Writing the above equation of motion in matrix-vector form for all particles yields

$$\frac{\mathrm{d}\mathbf{Q}}{\mathrm{d}t} = \tilde{DF}^{-1}\mathbf{V}, \tag{3.64}$$

$$\frac{\mathrm{d}\mathbf{V}}{\mathrm{d}t} = \tilde{DF}^{-\top}\hat{\mathbb{B}}\tilde{G}^{-1}\mathbb{P}^{1\top}\mathbf{u} - \tilde{DF}^{-\top}\hat{\mathbb{B}}\tilde{DF}^{-1}(\mathbf{q}_k)\mathbf{V}. \tag{3.65}$$

3.4 Hamiltonian system

From now on, we restrict ourselves for the moment on the case without control variate, i.e. $M_0 = 0$. To write down the semi-discrete system in Hamiltonian form, let us introduce the discrete Hamiltonian

$$\mathcal{H}_h := \frac{1}{2}\left((*\rho^3_{\mathrm{eq}}) \wedge \tilde{U}^1_h, \tilde{U}^1_h\right) + \frac{1}{2}(\tilde{B}^2_h, \tilde{B}^2_h) + \frac{1}{2}\int_{\hat{\Omega}} \epsilon_{\mathrm{h},123}\mathrm{d}^3q \tag{3.66}$$

$$= \frac{1}{2}\mathbf{u}^\top\mathcal{A}\mathbf{u} + \frac{1}{2}\mathbf{b}^\top\mathbb{M}^2\mathbf{b} + \frac{1}{2}\mathbf{V}^\top\mathbb{W}\mathbf{V}. \tag{3.67}$$

With this we can formulate the semi-discrete system in a 4×4 block structure:

$$\frac{\mathrm{d}}{\mathrm{d}t}\begin{pmatrix}\mathbf{u}\\ \mathbf{b}\\ \mathbf{Q}\\ \mathbf{V}\end{pmatrix} = \mathbb{J}(\mathbf{b}, \mathbf{Q})\nabla\mathcal{H} = \mathbb{J}(\mathbf{b}, \mathbf{Q})\begin{pmatrix}\mathcal{A}\mathbf{u}\\ \mathbb{M}^2\mathbf{b}\\ 0\\ \mathbb{W}\mathbf{V}\end{pmatrix} \tag{3.68}$$

We end up with an antisymmetric Poisson matrix meaning that the discrete Hamiltonian is conserved.

4 Time integration

4.1 Poisson splitting

We split the Poisson matrix into antisymmetric sub-systems such that each sub-system again defines a Hamiltonian system

$$\frac{\mathrm{d}}{\mathrm{d}t}\begin{pmatrix}\mathbf{u}\\ \mathbf{b}\\ \mathbf{Q}\\ \mathbf{V}\end{pmatrix} = \begin{pmatrix}\mathbb{J}_{11}(\mathbf{b}, \mathbf{Q}) & \mathbb{J}_{12} & 0 & \mathbb{J}_{14}(\mathbf{b}, \mathbf{Q})\\ -\mathbb{J}_{12}^\top & 0 & 0 & 0\\ 0 & 0 & 0 & \mathbb{J}_{34}(\mathbf{Q})\\ -\mathbb{J}_{14}^\top(\mathbf{b}, \mathbf{Q}) & 0 & -\mathbb{J}_{34}^\top(\mathbf{Q}) & \mathbb{J}_{44}(\mathbf{b}, \mathbf{Q})\end{pmatrix}\begin{pmatrix}\mathcal{A}\mathbf{u}\\ \mathbb{M}^2\mathbf{b}\\ 0\\ \mathbb{W}\mathbf{V}\end{pmatrix}, \tag{4.1}$$

$$\mathbb{J}_{11}(\mathbf{b}, \mathbf{Q}) = -\mathcal{A}^{-1}\mathbb{P}_1(\mathbf{Q})\mathbb{W}\tilde{G}^{-1}(\mathbf{Q})\hat{\mathbb{B}}(\mathbf{b}, \mathbf{Q})\tilde{G}^{-1}(\mathbf{Q})\mathbb{P}_1^\top(\mathbf{Q})\mathcal{A}^{-1}, \tag{4.2}$$

$$\mathbb{J}_{12} = \mathcal{A}^{-1}\mathcal{T}^\top\mathbb{C}^\top, \tag{4.3}$$

$$\mathbb{J}_{14}(\mathbf{b}, \mathbf{Q}) = \mathcal{A}^{-1}\mathbb{P}_1(\mathbf{Q})\tilde{G}^{-1}(\mathbf{Q})\hat{\mathbb{B}}(\mathbf{b}, \mathbf{Q})\tilde{DF}^{-1}(\mathbf{Q}), \tag{4.4}$$

$$\mathbb{J}_{34}(\mathbf{Q}) = \tilde{DF}^{-1}(\mathbf{Q})\mathbb{W}^{-1}, \tag{4.5}$$

$$\mathbb{J}_{44}(\mathbf{Q}) = -\tilde{DF}^{-\top}(\mathbf{Q})\hat{\mathbb{B}}(\mathbf{b}, \mathbf{Q})\tilde{DF}^{-1}(\mathbf{Q})\mathbb{W}^{-1}. \tag{4.6}$$

Sub-step 1 The first sub-system reads

$$\dot{\mathbf{u}} = \mathbb{J}_{11}(\mathbf{b}, \mathbf{Q})\mathcal{A}\mathbf{u}, \tag{4.7}$$
$$\dot{\mathbf{b}} = 0, \tag{4.8}$$
$$\dot{\mathbf{Q}} = 0, \tag{4.9}$$
$$\dot{\mathbf{V}} = 0. \tag{4.10}$$

We solve the this equation with the energy-preserving Crank-Nicolson method:

$$\frac{\mathbf{u}^{n+1} - \mathbf{u}^n}{\Delta t} = \mathbb{J}_{11}(\mathbf{b}^n, \mathbf{Q}^n)\mathcal{A}\frac{\mathbf{u}^n + \mathbf{u}^{n+1}}{2}. \tag{4.11}$$
$$\Leftrightarrow \quad \left(\mathbb{I} - \frac{\Delta t}{2}\mathbb{J}_{11}(\mathbf{b}^n, \mathbf{Q}^n)\mathcal{A}\right)\mathbf{u}^{n+1} = \left(\mathbb{I} + \frac{\Delta t}{2}\mathbb{J}_{11}(\mathbf{b}^n, \mathbf{Q}^n)\mathcal{A}\right)\mathbf{u}^n. \tag{4.12}$$

To avoid multiple matrix inversions, we multiply everything with $\mathcal{A}$ from the left to obtain

$$\left(\mathcal{A} - \frac{\Delta t}{2}\mathcal{A}\mathbb{J}_{11}(\mathbf{b}^n, \mathbf{Q}^n)\mathcal{A}\right)\mathbf{u}^{n+1} = \left(\mathcal{A} + \frac{\Delta t}{2}\mathcal{A}\mathbb{J}_{11}(\mathbf{b}^n, \mathbf{Q}^n)\mathcal{A}\right)\mathbf{u}^n. \tag{4.13}$$

We denote the corresponding integrator by $\Phi^1_{\Delta t}$.

Sub-step 2 The second sub-system reads

$$\dot{\mathbf{u}} = \mathbb{J}_{12}\mathbb{M}^2\mathbf{b}, \tag{4.14}$$
$$\dot{\mathbf{b}} = -\mathbb{J}_{12}^\top\mathcal{A}\mathbf{u}, \tag{4.15}$$
$$\dot{\mathbf{Q}} = 0, \tag{4.16}$$
$$\dot{\mathbf{V}} = 0. \tag{4.17}$$

We again solve this system with an energy-preserving Crank-Nicolson method:

$$\begin{pmatrix} \mathcal{A} & -\frac{\Delta t}{2}\mathcal{T}^\top\mathbb{C}^\top\mathbb{M}^2 \\ \frac{\Delta t}{2}\mathbb{C}\mathcal{T} & \mathbb{I} \end{pmatrix}\begin{pmatrix}\mathbf{u}^{n+1}\\ \mathbf{b}^{n+1}\end{pmatrix} = \begin{pmatrix} \mathcal{A} & \frac{\Delta t}{2}\mathcal{T}^\top\mathbb{C}^\top\mathbb{M}^2 \\ -\frac{\Delta t}{2}\mathbb{C}\mathcal{T} & \mathbb{I} \end{pmatrix}\begin{pmatrix}\mathbf{u}^{n}\\ \mathbf{b}^{n}\end{pmatrix}. \tag{4.18}$$

Using the Schur complement $S := \mathcal{A} + \frac{\Delta t^2}{4}\mathcal{T}^\top\mathbb{C}^\top\mathbb{M}^2\mathbb{C}\mathcal{T}$, we can calculate the in inverse of the matrix on the left-hand side which we can then multiply with the matrix on the right-hand side:

$$\begin{pmatrix} \mathcal{S}^{-1} & \frac{\Delta t}{2}\mathcal{S}^{-1}\mathcal{T}^\top\mathbb{C}^\top\mathbb{M}^2 \\ -\frac{\Delta t}{2}\mathbb{C}\mathcal{T}S^{-1} & \mathbb{I} - \frac{\Delta t^2}{4}\mathbb{C}\mathcal{T}\mathcal{S}^{-1}\mathcal{T}^\top\mathbb{C}^\top\mathbb{M}^2 \end{pmatrix}\begin{pmatrix} \mathcal{A} & \frac{\Delta t}{2}\mathcal{T}^\top\mathbb{C}^\top\mathbb{M}^2 \\ -\frac{\Delta t}{2}\mathbb{C}\mathcal{T} & \mathbb{I} \end{pmatrix} = \tag{4.19}$$

$$= \begin{pmatrix} \mathcal{S}^{-1}\mathcal{A} - \frac{\Delta t^2}{4}\mathcal{S}^{-1}\mathcal{T}^\top\mathbb{C}^\top\mathbb{M}^2\mathbb{C}\mathcal{T} & \Delta t\mathcal{S}^{-1}\mathcal{T}^\top\mathbb{C}^\top\mathbb{M}^2 \\ -\frac{\Delta t}{2}\mathbb{C}\mathcal{T}S^{-1}\mathcal{A} - \frac{\Delta t}{2}\mathbb{C}\mathcal{T} + \frac{\Delta t^3}{8}\mathbb{C}\mathcal{T}\mathcal{S}^{-1}\mathcal{T}^\top\mathbb{C}^\top\mathbb{M}^2\mathbb{C}\mathcal{T} & \mathbb{I} - \frac{\Delta t^2}{2}\mathbb{C}\mathcal{T}\mathcal{S}^{-1}\mathcal{T}^\top\mathbb{C}^\top\mathbb{M}^2 \end{pmatrix} \tag{4.20}$$

$$\Rightarrow \quad \mathbf{u}^{n+1} = \mathcal{S}^{-1}\left[\left(\mathcal{A} - \frac{\Delta t^2}{4}\mathcal{T}^\top\mathbb{C}^\top\mathbb{M}^2\mathbb{C}\mathcal{T}\right)\mathbf{u}^n + \Delta t\mathcal{T}^\top\mathbb{C}^\top\mathbb{M}^2\mathbf{b}^n\right] \tag{4.21}$$

$$\Rightarrow \quad \mathbf{b}^{n+1} = \mathbf{b}^n - \frac{\Delta t}{2}\mathbb{C}\mathcal{T}\left(\mathbf{u}^n + \mathcal{S}^{-1}\mathcal{A}\mathbf{u}^n - \frac{\Delta t^2}{2}\mathcal{S}^{-1}\mathcal{T}^\top\mathbb{C}^\top\mathbb{M}^2\mathbb{C}\mathcal{T}\mathbf{u}^n + \Delta t\mathcal{S}^{-1}\mathcal{T}^\top\mathbb{C}^\top\mathbb{M}^2\mathbf{b}^n\right) \tag{4.22}$$

$$= \mathbf{b}^n - \frac{\Delta t}{2}\mathbb{C}\mathcal{T}(\mathbf{u}^n + \mathbf{u}^{n+1}) \tag{4.23}$$

We immediately see that the update for $\mathbf{b}$ preserves the divergence-free constraint. We denote the corresponding integrator by $\Phi^2_{\Delta t}$.

Sub-step 3 The third sub-system reads

$$\dot{\mathbf{u}} = \mathbb{J}_{14}(\mathbf{b}, \mathbf{Q})\mathbb{W}\mathbf{V}, \tag{4.24}$$
$$\dot{\mathbf{b}} = 0, \tag{4.25}$$
$$\dot{\mathbf{Q}} = 0, \tag{4.26}$$
$$\dot{\mathbf{V}} = -\mathbb{J}_{14}^{\top}(\mathbf{b}, \mathbf{Q})\mathcal{A}\mathbf{u}. \tag{4.27}$$

We solve this system in the same way as before. Since $\mathbf{b}$ and $\mathbf{Q}$ do not change in this step, the same is true for the matrix $\mathbb{J}_{14}$. Hence $\mathbb{J}_{14} = \mathbb{J}_{14}(\mathbf{b}^n, \mathbb{Q}^n)$ and we have

$$\begin{pmatrix} \mathcal{A} & -\frac{\Delta t}{2}\mathcal{A}\mathbb{J}_{14}\mathbb{W} \\ \frac{\Delta t}{2}\mathbb{J}_{14}^{\top}\mathcal{A} & \mathbb{I} \end{pmatrix} \begin{pmatrix} \mathbf{u}^{n+1} \\ \mathbf{V}^{n+1} \end{pmatrix} = \begin{pmatrix} \mathcal{A} & \frac{\Delta t}{2}\mathcal{A}\mathbb{J}_{14}\mathbb{W} \\ -\frac{\Delta t}{2}\mathbb{J}_{14}^{\top}\mathcal{A} & \mathbb{I} \end{pmatrix} \begin{pmatrix} \mathbf{u}^{n} \\ \mathbf{V}^{n} \end{pmatrix}. \tag{4.28}$$

Using once more the Schur complement $\mathcal{S}^{-1} := \mathcal{A} + \frac{\Delta t^2}{4}\mathcal{A}\mathbb{J}_{14}\mathbb{W}\mathbb{J}_{14}^{\top}\mathcal{A}$ yields

$$\mathbf{u}^{n+1} = \mathcal{S}^{-1}\left[\left(\mathcal{A} - \frac{\Delta t^2}{4}\mathcal{A}\mathbb{J}_{14}\mathbb{W}\mathbb{J}_{14}^{\top}\mathcal{A}\right)\mathbf{u}^n + \Delta t\mathcal{A}\mathbb{J}_{14}\mathbb{W}\mathbf{V}^n\right], \tag{4.29}$$
$$\mathbf{V}^{n+1} = \mathbf{V}^n - \frac{\Delta t}{2}\mathbb{J}_{14}^{\top}\mathcal{A}(\mathbf{u}^n + \mathbf{u}^{n+1}) \tag{4.30}$$

We denote the corresponding integrator by $\Phi_{\Delta t}^3$.

Sub-step 4 The fourth sub-system reads

$$\dot{\mathbf{u}} = 0, \tag{4.31}$$
$$\dot{\mathbf{b}} = 0, \tag{4.32}$$
$$\dot{\mathbf{Q}} = \mathbb{J}_{34}(\mathbf{Q})\mathbb{W}\mathbf{V}, \tag{4.33}$$
$$\dot{\mathbf{V}} = 0. \tag{4.34}$$

Using again a Crank-Nicolson approximation for particle k yields

$$\mathbf{q}_k^{n+1} = \mathbf{q}_k^n + \frac{\Delta t}{2}(DF^{-1}(\mathbf{q}_k^n) + DF^{-1}(\mathbf{q}_k^{n+1}))\mathbf{v}_k^n, \tag{4.35}$$

which can be solved for $\mathbf{q}^{n+1}$ using a fix point iteration. We denote the corresponding integrator by $\Phi_{\Delta t}^4$.

Sub-step 5 The fifth sub-system reads

$$\dot{\mathbf{u}} = 0, \tag{4.36}$$
$$\dot{\mathbf{b}} = 0, \tag{4.37}$$
$$\dot{\mathbf{Q}} = 0, \tag{4.38}$$
$$\dot{\mathbf{V}} = \mathbb{J}_{44}(\mathbf{b}, \mathbf{Q})\mathbb{W}\mathbf{V}. \tag{4.39}$$

Using again a Crank-Nicolson approximation for particle k yields

$$\left(\mathbb{I} + \frac{\Delta t}{2}DF^{-\top}(\mathbf{q}_k^n)\hat{\mathbb{B}}_h(\mathbf{q}_k^n)DF^{-1}(\mathbf{q}_k^n)\right)\mathbf{v}_k^{n+1} = \left(\mathbb{I} - \frac{\Delta t}{2}DF^{-\top}(\mathbf{q}_k^n)\hat{\mathbb{B}}_h(\mathbf{q}_k^n)DF^{-1}(\mathbf{q}_k^n)\right)\mathbf{v}_k^n. \tag{4.40}$$

We denote the corresponding integrator by $\Phi_{\Delta t}^5$.

5 Dispersion relation

In this section we derive the dispersion relation for wave propagation parallel to an external, uniform magnetic field $\mathbf{B} = B_0\mathbf{e}_z$. Although we have $\mathbf{E} = -\mathbf{U}\times\mathbf{B}$ in ideal MHD, we assume for the moment a general electric field. With this, linearization of the Vlasov equation about an homogeneous (in space) equilibrium $f_\mathrm{h}^0 = f_\mathrm{h}^0(v_\parallel, v_\perp)$ yields

$$\frac{\partial f_\mathrm{h}}{\partial t} + \mathbf{v}\cdot\nabla f_\mathrm{h} + \Omega_\mathrm{ch}(\mathbf{v}\times\mathbf{e}_z)\cdot\nabla_\mathbf{v} f_\mathrm{h} = -\frac{q_\mathrm{h}}{m_\mathrm{h}}(\mathbf{E}+\mathbf{v}\times\mathbf{B})\cdot\nabla_\mathbf{v} f_\mathrm{h}^0. \tag{5.1}$$

The solution of this equation in Fourier space leads to an Ohm's law of the form

$$\hat{\mathbf{j}}_\mathrm{h} = \begin{pmatrix} -i\frac{q_\mathrm{h}^2}{m_\mathrm{h}}\int\frac{v_\perp(\omega-kv_\parallel)\hat{G}f_\mathrm{h}^0}{2\Omega_+\Omega_-}\mathrm{d}^3v & \frac{q_\mathrm{h}^2}{m_\mathrm{h}}\Omega_\mathrm{ch}\int\frac{v_\perp\hat{G}f_\mathrm{h}^0}{2\Omega_+\Omega_-}\mathrm{d}^3v & 0 \\ -\frac{q_\mathrm{h}^2}{m_\mathrm{h}}\Omega_\mathrm{ch}\int\frac{v_\perp\hat{G}f_\mathrm{h}^0}{2\Omega_+\Omega_-}\mathrm{d}^3v & -i\frac{q_\mathrm{h}^2}{m_\mathrm{h}}\int\frac{v_\perp(\omega-kv_\parallel)\hat{G}f_\mathrm{h}^0}{2\Omega_+\Omega_-}\mathrm{d}^3v & 0 \\ 0 & 0 & -i\frac{q_\mathrm{h}^2}{m_\mathrm{h}}\int\frac{v_\parallel\partial_\parallel f_\mathrm{h}^0}{\omega-kv_\parallel}\mathrm{d}^3v \end{pmatrix}\hat{\mathbf{E}} = \sigma_\mathrm{h}(k,\omega)\hat{\mathbf{E}}, \tag{5.2}$$

where $\hat{G} = \partial/\partial v_\perp + k(v_\perp\partial/\partial v_\parallel - v_\parallel\partial/\partial v_\perp)/\omega$ is a differential operator measuring the anisotropy of the distribution function and velocity space and $\Omega_\pm = \omega - kv_\parallel \pm\Omega_\mathrm{ce}$ denote the frequencies of resonant particles. We make now use of the fact that $\hat{\mathbf{E}} = -B_0\hat{\mathbf{U}}\times\mathbf{e}_z$ in ideal MHD. This yields a pure transverse current with components

$$\hat{j}_{\mathrm{h}x} = -\sigma_{\mathrm{h}xx}B_0U_y + \sigma_{\mathrm{h}xy}B_0U_x \tag{5.3}$$

$$\hat{j}_{\mathrm{h}y} = -\sigma_{\mathrm{h}yx}B_0U_y + \sigma_{\mathrm{h}yy}B_0U_x. \tag{5.4}$$

The momentum balance equation then reads

$$-i\omega\hat{\mathbf{U}} + i\frac{v_\mathrm{A}^2k^2}{\omega}\hat{\mathbf{U}}_\perp + i\frac{c_\mathrm{S}^2k^2}{\omega}\mathbf{e}_z\hat{U}_\parallel = \frac{Z_\mathrm{h}\nu_\mathrm{h}\Omega_\mathrm{ch}}{A_\mathrm{MHD}}\hat{\mathbf{U}}\times\mathbf{e}_z + \frac{B_0}{\rho_\mathrm{eq}}(\mathbf{e}_z\times\hat{\mathbf{j}}_\mathrm{h}), \tag{5.5}$$

where we approximated the bulk mass density by the ion contribution $\rho_\mathrm{eq} = A_\mathrm{MHD}m_\mathrm{i}n_0$, Z_h is the hot ion charge number and $\nu_\mathrm{h} = n_\mathrm{h0}/n_0$ is the the ratio of the equilibrium bulk and energetic ion number densities. Writing everything in terms of the bulk velocity yields the linear system

$$\begin{pmatrix} \omega^2 - v_\mathrm{A}^2k^2 + iv_\mathrm{A}^2\sigma_{\mathrm{h}yy}\omega & i\left(-\frac{Z_\mathrm{h}\nu_\mathrm{h}\Omega_\mathrm{ch}\omega}{A_\mathrm{MHD}} - v_\mathrm{A}^2\sigma_{\mathrm{h}yx}\omega\right) & 0 \\ -i\left(-\frac{Z_\mathrm{h}\nu_\mathrm{h}\Omega_\mathrm{ch}\omega}{A_\mathrm{MHD}} + v_\mathrm{A}^2\sigma_{\mathrm{h}xy}\omega\right) & \omega^2 - v_\mathrm{A}^2k^2 + iv_\mathrm{A}^2\sigma_{\mathrm{h}xx}\omega & 0 \\ 0 & 0 & \omega^2 - c_\mathrm{S}^2k^2 \end{pmatrix}\begin{pmatrix}\hat{U}_x\\ \hat{U}_y\\ \hat{U}_\parallel\end{pmatrix} = 0. \tag{5.6}$$

The structure of this system immediately reveals that we deal with circularly polarized waves in perpendicular direction characterized by $iU_x/U_y = \pm1$ for R/L-waves, respectively. This leads to the dispersion relation

$$D_\mathrm{R/L}(k,\omega) = 1 - \frac{v_\mathrm{A}^2k^2}{\omega^2} + \frac{iv_\mathrm{A}^2\sigma_{\mathrm{h}xx}}{\omega} \pm \frac{Z_\mathrm{h}\nu_\mathrm{h}\Omega_\mathrm{ch}}{A_\mathrm{MHD}\omega} \mp \frac{v_\mathrm{A}^2\sigma_{\mathrm{h}xy}}{\omega} \tag{5.7}$$

$$= 1 - \frac{v_\mathrm{A}^2k^2}{\omega^2} \pm \frac{Z_\mathrm{h}\nu_\mathrm{h}\Omega_\mathrm{ch}}{A_\mathrm{MHD}\omega} + \frac{\nu_\mathrm{h}\Omega_\mathrm{ch}^2Z_\mathrm{h}^2}{A_\mathrm{h}A_\mathrm{MHD}\omega}\int\frac{v_\perp}{2}\frac{\hat{G}F_\mathrm{h}^0}{\omega - kv_\parallel \pm\Omega_\mathrm{ch}}\mathrm{d}^3v = 0. \tag{5.8}$$

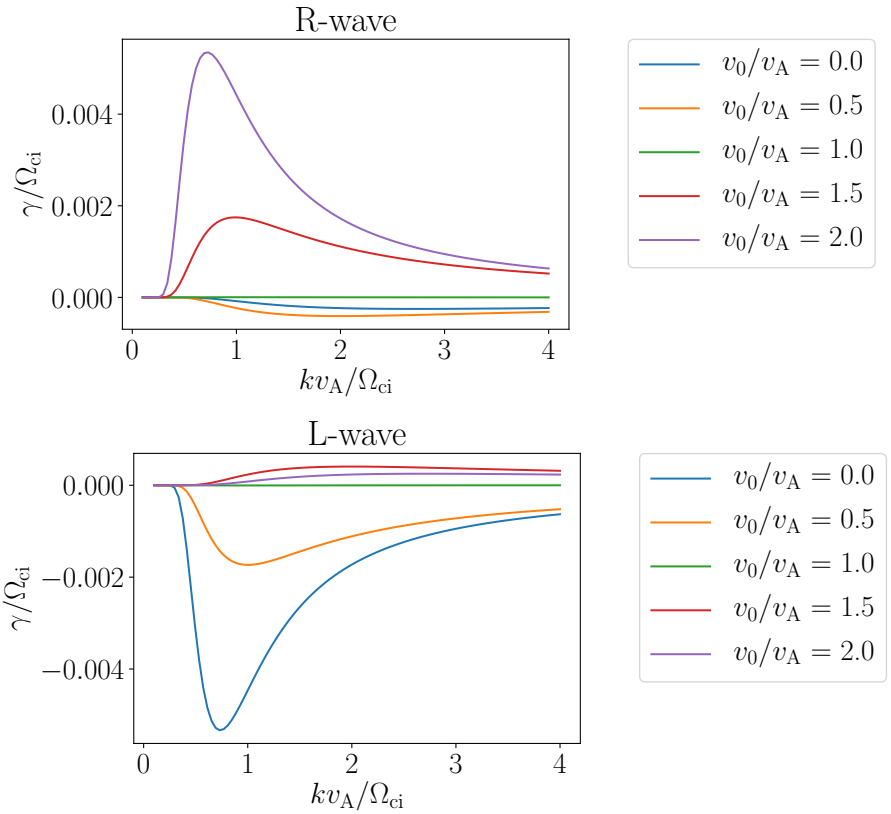

Figure 3: Growth rates for different shifts of the Maxwellian

Assuming a shifted, isotropic Maxwellian of the form

$$F_{\rm h}^0 = \frac{1}{\pi^{3/2} v_{\rm th}^3} \exp\left(-\frac{(v_\parallel - v_0)^2 + v_\perp^2}{v_{\rm th}^2}\right) \tag{5.9}$$

$$\Rightarrow \frac{\partial F_{\rm h}^0}{\partial v_\parallel} = -F_{\rm h}^0 \frac{2}{v_{\rm th}^2}(v_\parallel - v_0) \tag{5.10}$$

$$\Rightarrow \frac{\partial F_{\rm h}^0}{\partial v_\perp} = -F_{\rm h}^0 \frac{2}{v_{\rm th}^2} v_\perp \tag{5.11}$$

$$\Rightarrow \hat{G} F_{\rm h}^0 = -F_{\rm h}^0 \frac{2}{v_{\rm th}^2} v_\perp + \frac{k}{\omega} F_{\rm h}^0 \frac{2}{v_{\rm th}^2} v_\perp v_0 = F_{\rm h}^0 \frac{2 v_\perp}{v_{\rm th}^2}\left(\frac{k v_0}{\omega} - 1\right) \tag{5.12}$$

$$\Rightarrow \pi \int_0^\infty \frac{1}{\pi^{3/2} v_{\rm th}^3} \begin{pmatrix} 1 \\ v_\perp \\ v_\perp^2 \\ v_\perp^3 \end{pmatrix} \exp\left(-\frac{v_\perp^2}{v_{\rm th}^2}\right) {\rm d}v_\perp = \begin{pmatrix} 1/(2v_{\rm th}^2) \\ 1/(2v_{\rm th}\sqrt{\pi}) \\ 1/4 \\ v_{\rm th}/(2\sqrt{\pi}) \end{pmatrix}, \tag{5.13}$$

leads to

$$D_{\rm R/L}(k,\omega) = 1 - \frac{v_{\rm A}^2 k^2}{\omega^2} \pm \frac{Z_{\rm h} \nu_{\rm h} \Omega_{\rm ch}}{A_{\rm MHD}\omega} + \frac{\nu_{\rm h} \Omega_{\rm ch}^2 Z_{\rm h}^2}{A_{\rm h} A_{\rm MHD} \omega^2} \frac{\omega - k v_0}{k v_{\rm th}} Z(\xi^\pm), \tag{5.14}$$

where Z is the plasma dispersion function and $\xi\pm = (\omega - k v_0 \pm \Omega_{\rm ch})/(k v_{\rm th})$.

References

[1] D. Arnold, R. Falk, and R. Winther. Finite element exterior calculus: from Hodge theory to numerical stability. *Bulletin of the American mathematical society*, 47(2):281–354, 2010.

[2] D. N. Arnold. *Finite element exterior calculus*, volume 93. SIAM, 2018.

[3] D. N. Arnold, R. S. Falk, and R. Winther. Finite element exterior calculus, homological techniques, and applications. *Acta numerica*, 15:1–155, 2006.

[4] E. Belova, R. Denton, and A. Chan. Hybrid simulations of the effects of energetic particles on low-frequency MHD waves. *Journal of Computational Physics*, 136(2):324–336, 1997.

[5] S. Briguglio, G. Vlad, F. Zonca, and C. Kar. Hybrid magnetohydrodynamic-gyrokinetic simulation of toroidal Alfvén modes. *Physics of Plasmas*, 2(10):3711–3723, 1995.

[6] J. W. Burby and C. Tronci. Variational approach to low-frequency kinetic-MHD in the current coupling scheme. *Plasma Physics and Controlled Fusion*, 59(4):045013, 2017.

[7] G. Chen and L. Chacón. An energy-and charge-conserving, nonlinearly implicit, electromagnetic 1D-3V Vlasov–Darwin particle-in-cell algorithm. *Computer Physics Communications*, 185(10):2391–2402, 2014.

[8] L. Chen and F. Zonca. Physics of Alfvén waves and energetic particles in burning plasmas. *Reviews of Modern Physics*, 88(1):015008, 2016.

[9] E. Evstatiev and B. Shadwick. Variational formulation of particle algorithms for kinetic plasma simulations. *Journal of Computational Physics*, 245:376–398, 2013.

[10] Y. He, H. Qin, Y. Sun, J. Xiao, R. Zhang, and J. Liu. Hamiltonian time integrators for Vlasov-Maxwell equations. *Physics of Plasmas*, 22(12):124503, 2015.

[11] Y. He, Y. Sun, H. Qin, and J. Liu. Hamiltonian particle-in-cell methods for Vlasov-Maxwell equations. *Physics of Plasmas*, 23(9):092108, 2016.

[12] W. Heidbrink. Basic physics of Alfvén instabilities driven by energetic particles in toroidally confined plasmas. *Physics of Plasmas*, 15(5):055501, 2008.

[13] A. Könies, S. Briguglio, N. Gorelenkov, T. Fehér, M. Isaev, P. Lauber, A. Mishchenko, D. Spong, Y. Todo, W. Cooper, et al. Benchmark of gyrokinetic, kinetic MHD and gyrofluid codes for the linear calculation of fast particle driven TAE dynamics. *Nuclear Fusion*, 58(12):126027, 2018.

[14] M. Kraus, K. Kormann, P. J. Morrison, and E. Sonnendrücker. GEMPIC: Geometric electromagnetic particle-in-cell methods. *Journal of Plasma Physics*, 83(4), 2017.

[15] P. Lauber. Super-thermal particles in hot plasmas—Kinetic models, numerical solution strategies, and comparison to tokamak experiments. *Physics Reports*, 533(2):33–68, 2013.

[16] P. J. Morrison. Structure and structure-preserving algorithms for plasma physics. *Physics of Plasmas*, 24(5):055502, 2017.

[17] P. J. Morrison and J. M. Greene. Noncanonical Hamiltonian density formulation of hydrodynamics and ideal magnetohydrodynamics. *Physical Review Letters*, 45(10):790, 1980.

[18] W. Park, E. Belova, G. Fu, X. Tang, H. Strauss, and L. Sugiyama. Plasma simulation studies using multilevel physics models. *Physics of Plasmas*, 6(5):1796–1803, 1999.

[19] H. Qin, J. Liu, J. Xiao, R. Zhang, Y. He, Y. Wang, Y. Sun, J. W. Burby, L. Ellison, and Y. Zhou. Canonical symplectic particle-in-cell method for long-term large-scale simulations of the Vlasov–Maxwell equations. *Nuclear Fusion*, 56(1):014001, 2015.

[20] J. Squire, H. Qin, and W. M. Tang. Geometric integration of the Vlasov-Maxwell system with a variational particle-in-cell scheme. *Physics of Plasmas*, 19(8):084501, 2012.

[21] Y. Todo and T. Sato. Linear and nonlinear particle-magnetohydrodynamic simulations of the toroidal Alfvén eigenmode. *Physics of plasmas*, 5(5):1321–1327, 1998.

[22] C. Tronci. Hamiltonian approach to hybrid plasma models. *Journal of Physics A: Mathematical and Theoretical*, 43(37):375501, 2010.

[23] X. Wang, S. Briguglio, L. Chen, C. Di Troia, G. Fogaccia, G. Vlad, and F. Zonca. An extended hybrid magnetohydrodynamics gyrokinetic model for numerical simulation of shear Alfvén waves in burning plasmas. *Physics of Plasmas*, 18(5):052504, 2011.

[24] J. Xiao and H. Qin. Field theory and a structure-preserving geometric particle-in-cell algorithm for drift wave instability and turbulence. *Nuclear Fusion*, 59(10):106044, 2019.

[25] J. XIAO, H. QIN, and J. LIU. Structure-preserving geometric particle-in-cell methods for Vlasov-Maxwell systems. *Plasma Science and Technology*, 20(11):110501, sep 2018.

[26] J. Xiao, H. Qin, J. Liu, and R. Zhang. Local energy conservation law for a spatially-discretized Hamiltonian Vlasov-Maxwell system. *Physics of Plasmas*, 24(6):062112, 2017.